*Int. J. Electrochem. Sci.*, 16 **(2021)** Article ID: 210450, doi: 10.20964/2021.04.39

International Journal of
ELECTROCHEMICAL
SCIENCE
www.electrochemsci.org

# A Simple Strategy for the Simultaneous Determination of Dopamine, Uric Acid, L-Tryptophan and Theophylline Based on a Carbon Dots Modified Electrode

*Ziwei Wang, Rui An, Yuxuan Dai, Hongxia Luo*[*]

Department of Chemistry, Renmin University of China, Beijing 100872, China
[*]E-mail: luohx@ruc.edu.cn

*Received:* 2 December 2020 / *Accepted:* 27 January 2021 / *Published:* 28 February 2021

In this work, carbon dots (CDs) were produced by one-step ultrasound technology with glucose as the precursor. The effective synthesis of CDs was characterized by Raman spectroscopy and UV-visible spectra. The as-prepared CDs were fixed on a glassy carbon electrode (GCE) via electrochemical deposition to fabricate CDs/GCE, which simultaneously detected dopamine (DA), uric acid (UA), L-tryptophan (Trp) and theophylline (TP). With the differential pulse voltammetry technique, the oxidation peak currents of these four biomolecules were significantly enhanced on CDs/GCE compared to those on bare GCE. The potential differences of DA-UA, UA-Trp, and Trp-TP were computed as 145 mV, 381 mV, and 323 mV, respectively. The broad linear ranges were 0.5-50 μM for DA, 3-75 μM for UA, 1-65 μM for Trp and 10-200 μM for TP with limits of detection (LODs) of 0.007 μM, 0.011 μM, 0.11 μM and 0.33 μM (S/N = 3), respectively. The CD/GCE sensor had good stability and strong anti-interference ability and was applicable to detecting actual samples.

**Keywords:** Carbon dots; Glassy carbon electrode; Electrochemical sensing; Dopamine; Uric acid; L-tryptophan; Theophylline

## 1. INTRODUCTION

Monitoring the relevant biomolecules plays a vital role in early disease surveillance. Dopamine (DA) is the richest catecholamine neurotransmitter in the brain [1], and an imbalance in its concentration will affect the human nervous system, leading to Parkinson's disease, depression, schizophrenia and other diseases [2]. In the clinical diagnosis of some diseases, particularly gout, uric acid (UA) is a significant symbol [3]. UA is diffusely spread over the urine and blood of mammals, and it is a product of the purine metabolism [4]. L-tryptophan (Trp) is among the most crucial amino acids required for the biosynthesis of proteins and greatly affects the human metabolism [5]. Theophylline (TP) is a natural alkaloid because it can relax smooth muscles and is effectively used to clinically treat

bronchial asthma [6]. DA [7, 8], UA [9, 10], Trp [11] and TP [12-14] always coexist in human serum. Considering the importance of these four biomolecules, their efficacious and simultaneous identification has become more popular in different types of fields.

Two or more biomolecules in DA, UA, Trp, and TP have been discriminated on different electrodes. Chen et al. decorated poly(β-cyclodextrin) and CDs together on GCE to simultaneously and effectively detect DA, UA and Trp [15]. Yang et al. utilized a ferrocene derivative functional Au NP/CD nanocomposite and graphene to distinguish ascorbic acid (AA), DA, UA and acetaminophen (AC) [16]. After fabricating hemin-graphene oxide-pristine carbon nanotube complexes, Zhang et al. synchronously analyzed Trp, AA, UA, and DA [17]. Sun et al. reported an Au nanoparticle/$TiO_2$ nanoparticle/carbon nanotube composite biosensor, which was applied to sensitively concurrently discriminate AA, UA, DA, and Trp [18]. Yang et al. modified cetyltrimethylammonium bromide on GCE through electropolymerization, and a biosensor that can discriminate DA, UA, Trp and TP was successfully assembled [19]. Few studies simultaneously detected DA, UA, Trp and TP.

As an emerging zero-dimensional material, carbon dots (CDs) have attracted widespread attention during the past few years [20]. CDs have remarkable properties such as small size, excellent biocompatibility, environmental friendliness, low toxicity, abundant surface functional groups and low cost [21, 22]. Thus, CDs have been widely used in cell imaging [23], drug delivery [24], gene delivery [25] and fluorescence sensors [26]. Electrochemical methods can act as effective means for CD nanomaterials. Meanwhile, they can furnish mild reaction conditions, ease manipulation and increase cost effectiveness. As a result, CDs have served as electrochemical sensors [27] and commendably solved the trace detection of biomolecules, including AA, DA, UA [28], metanil yellow, curcumin [29], guanine, adenine [22], paracetamol, p-aminophenol [30], hydroquinone, catechol and resorcinol [31]. Hence, it is significant to utilize CDs on modified electrodes for electrochemical sensors.

In this work, CDs were synthesized by one-step ultrasound technology and decorated on the surface of GCE via electrochemical deposition to fabricate a CD/GCE. The synchronous electrochemical measurement of DA, UA, Trp and TP with enhanced electrochemical behaviors was finally realized on the CDs/GCE.

## 2. EXPERIMENT

### *2.1. Original materials and reagents*

Sigma-Aldrich Co. LLC provided DA and UA. Trp was from BIO BASIC INC. Both TP and glucose were from Aladdin Industrial Corporation. NaOH was provided by Yili Chemical (Beijing, China). $KH_2PO_4$ and $Na_2HPO_4$ comprised phosphate buffer solution (PBS, 0.1 M). The reagents in the experiments were of analytical grade.

### *2.2. Apparatus*

A CHI 660D workstation (Shanghai Chenhua, China) with a traditional three-electrode system was utilized to perform all electrochemical measurements containing cyclic voltammetry (CV), differential pulse voltammograms (DPV) and electrochemical impedance spectroscopy (EIS). The

proposed CDs/GCE was employed as the working electrode. An Ag/AgCl electrode and a platinum electrode acted as the reference electrode and counter electrode, respectively. The UV-visible spectra of the CDs and glucose were obtained by an ultraviolet-visible spectrophotometer (TU-1901). The Raman spectra (Xplora plus) analysis of CDs was recorded on a Raman spectrometer with a 532-nm laser [32]. The morphologies of GCE and CDs/GCE were obtained by scanning electron microscopy (SEM) (SU8010).

### *2.3. Production of CDs and CDs/GCE*

CDs were acquired by a one-step ultrasonic technique [33]. A moderate amount of glucose was mixed with 50 mL ultrapure water (Milli-Q, Millipore); then, a uniform and transparent solution (1 mol/L) was formed. Under stirring conditions, the pre-prepared NaOH solution (50 mL, 1 mol/L) was poured into the glucose solution [34]. After 4 h of ultrasound, the resulting mixture changed from clear transparency to deep reddish brown, which indicates the successful synthesis of CDs. Finally, the CD solution (pH 13.0) was diluted to 200 mL and stored at 4 °C for future experiments [33].

Prior to modification, the GCE was polished with 10 nm aluminum oxide powders and subsequently successively immersed in water and ethanol for ultrasonic cleaning. [35]. Then, the GCE was scanned in 10 mL CD solution from -0.8 ~ 0.8 V with 50 $mV \cdot s^{-1}$ for 50 cycles [36]. After gentle rinsing with ultrapure water, the resulting CDs/GCE was set aside to dry. Fig. 1 shows a schematic diagram of the analysis of CDs/GCE for the simultaneous determination of DA, UA, Trp and TP.

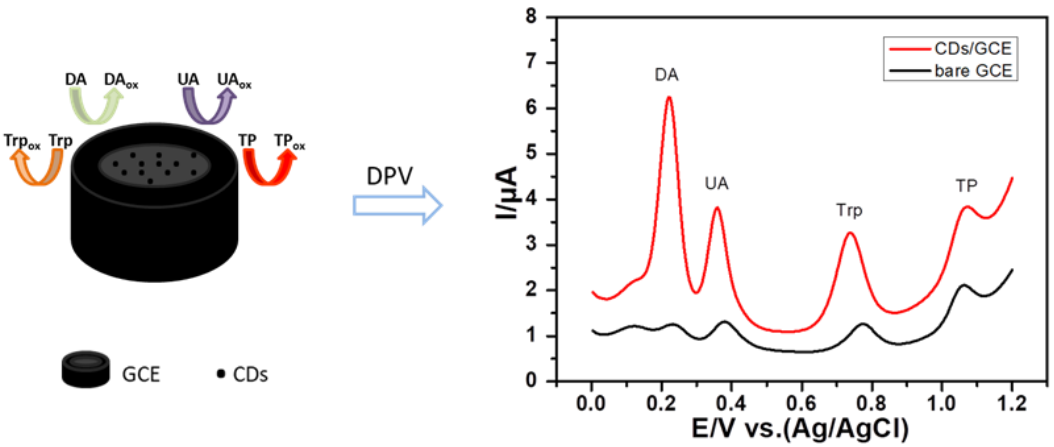


**Figure 1.** Schematic diagram of the analysis of CDs/GCE to synchronously detect DA, UA, Trp and TP.

## 3. RESULTS AND DISCUSSION

### *3.1. Characterization of CDs*

There was no obvious absorption peak in glucose within a certain wavelength range in the UV-

visible spectra (Fig. 2). Moreover, the CDs had a peak at 276 nm due to the π – π* transition [37], which was similar to polycyclic aromatic hydrocarbons [34].

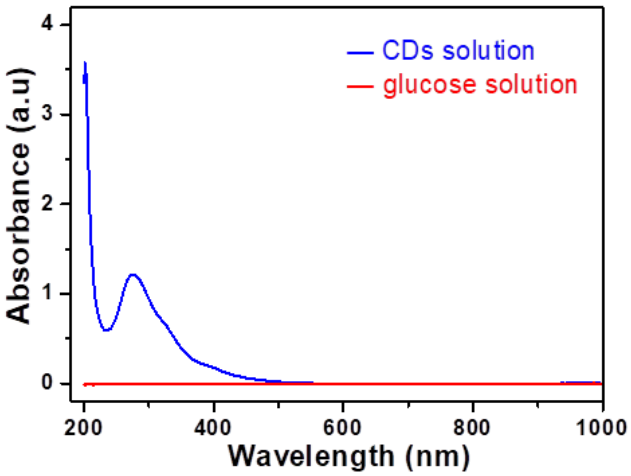


**Figure 2.** UV-visible spectra for aqueous solutions of glucose (red) and CDs (blue).

The obtained CDs were dried in air and studied using Raman spectrometry. As shown in Fig. 3, the D band (1347 $cm^{-1}$) and G band (1591 $cm^{-1}$) were observed as two distinct characteristic peaks of carbon, where the D band represents the disordered carbon structure ($sp^3$), and the G band represents the ordered graphite carbon ($sp^2$) [38]. This result proves the hybridization type of carbon in the prepared carbon dots.

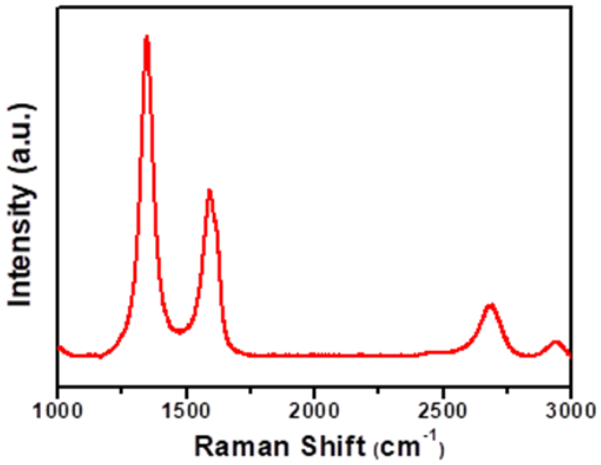


**Figure 3.** Raman spectra of CDs on GCE.

*3.2. Surface characterization of the CDs/GCE*

Fig. 4 illustrates the SEM images. Fig. 4A reveals a smooth surface, which conforms to the characterization of the bare GCE in the literature [39, 40]. Fig. 4B presents a totally different

morphology for CDs/GCE compared to the bare GCE, which testifies that the CDs had been faultlessly modified on the GCE. As visually observed, the modified CDs were very evenly distributed. Comparatively, the sizes of attached CDs were relatively uniform [41].

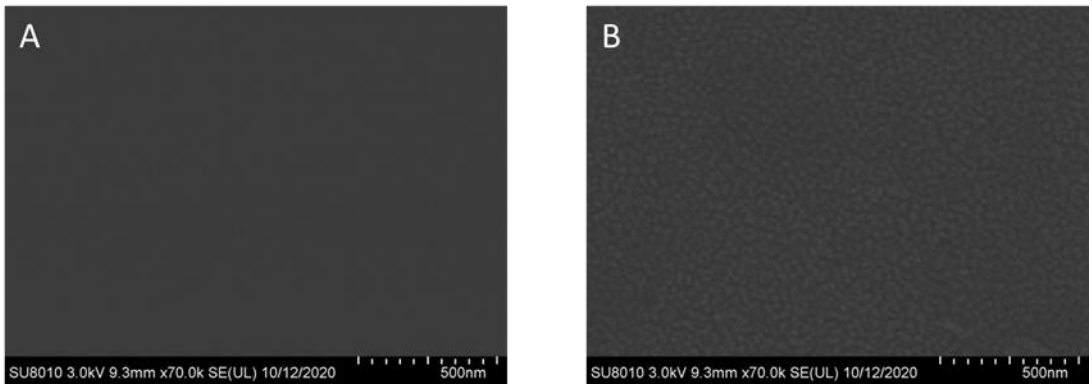


**Figure 4.** SEM images: (A) bare GCE; (B) CDs/GCE.

*3. 3. Electrochemical reactivity of the CDs/GCE*

Fig. 5A shows the EIS. The bare GCE had a tiny arc in the high-frequency region [42, 43], and its charge transfer resistance ($R_{ct}$) was approximately 285 Ω. However, after modifying the CDs on the surface of the GCE, the Nyquist plot consisted of a semicircle and a straight line with an $R_{ct}$ value of approximately 2000 Ω, which was attributed to the formation of the CD layer [44]. Comparatively, the signal of CDs/GCE (Fig. 5B) in the $[Fe(CN)_6]^{3-}$ solution with KCl visibly decreased.

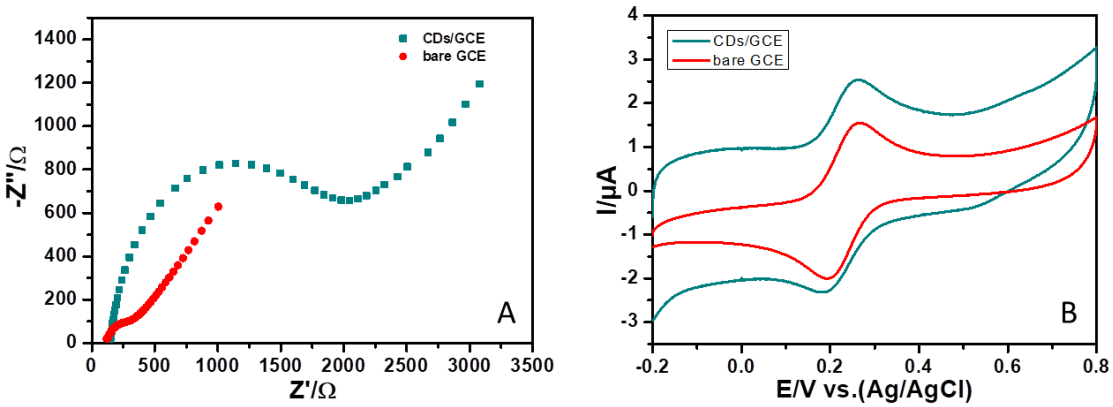


**Figure 5.** (A) Nyquist plots of CDs/GCE and bare GCE in 1 mM $[Fe(CN)_6]^{3-/4-}$ solution with 0.1 M KCl; (B) CV obtained at the CDs/GCE (green) and bare GCE (red) in 0.1 M KCl with 0.1 mM $[Fe(CN)_6]^{3-}$.

*3.4. Electrochemical performance of CDs/GCE for DA, UA, Trp and TP*

The electrochemical characteristics of CDs/GCE were determined by DPV. Fig. 6 shows the

DPV of CDs/GCE and bare GCE when the four biomolecules coexisted. When the DA concentration was low, it was difficult to detect the peak signal of DA on the bare GCE (black curve), while CDs/GCE significantly amplified the current signal of DA. In addition, the bare GCE could recognize and detect UA, Trp and TP, but the electrochemical signal was weak. However, the current signal of the three species was visually enhanced on CDs/GCE, which indicates that the CD modification is very effective.

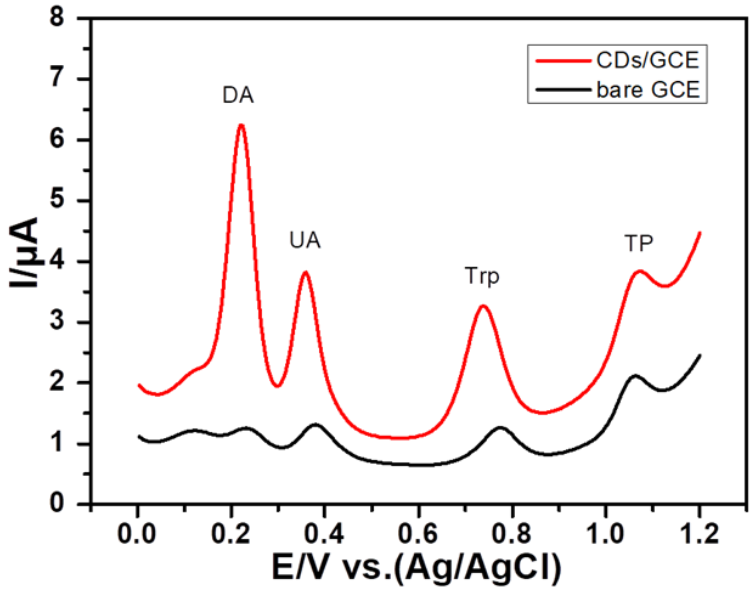


**Figure 6.** DPVs on CDs/GCE (red) and bare GCE (black) in 5 μM DA, 35 μM UA, 50 μM Trp and 60 μM TP (PBS 6.0).

### *3. 5. Optimization of parameters*

#### *3.5.1. The influence exerted by cycle numbers*

The GCE was cycled between -0.8 and +0.8 V in 50 mg/mL CD solution at 100 mV $s^{-1}$ for 30, 40, 50, and 60 cycles. The cycle numbers in the electrodeposition process directly affected the amount of CD modification and peak current signal. Hence, the effect of the cycle number was surveyed in PBS (pH 6.0) comprising 5 μM DA, 35 μM UA, 50 μM Trp and 60 μM TP using the DPV method, and the best result was obtained when 50 cycles were applied (Fig. 7).

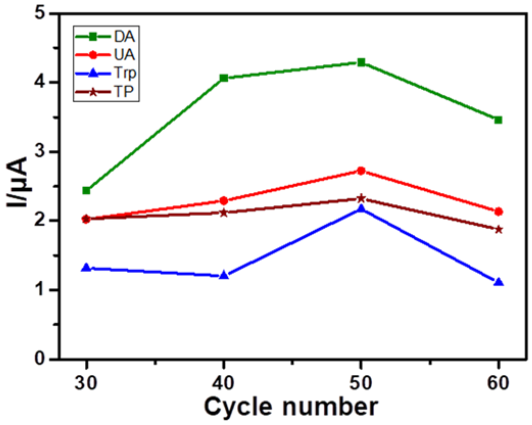


**Figure 7.** Relationship between current intensity and number of cycles of deposition.

*3.5.2. The influence exerted by pH value*

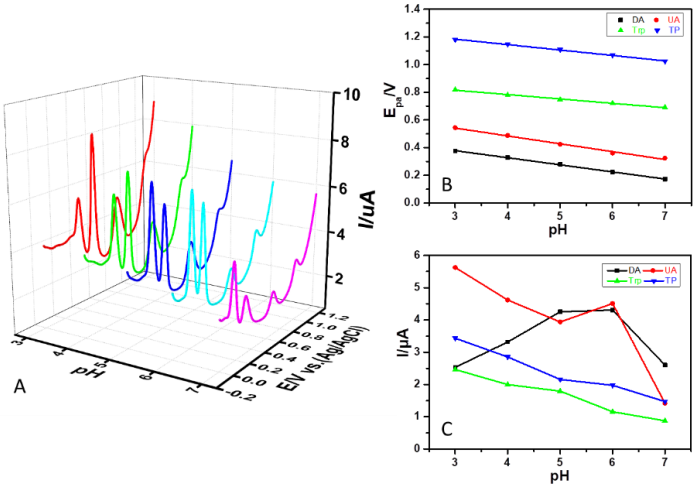


**Figure 8.** (A) DPVs of 5 μM DA, 40 μM UA, 20 μM Trp and 60 μM TP on CDs/GCE with various pH values (3.0-7.0). (B) Correlation between peak potential and pH. (C) Variation of the peak current with pH.

The pH value was optimized to simultaneously identify the above four compounds. Based on the CDs/GCE, the DPV method was performed with various pH values (Fig. 8A). Under each pH condition, the peak potential differences were not obvious, but under the condition of pH = 6.0, each peak type was relatively intuitionistic, especially for TP.

As directly observed in Fig. 8B, the peak potential responded to the change in pH value. The peak potentials of the four biomolecules decreased when the pH increased, which indicates that protons combined with oxidation products during the reaction. The corresponding linear regressions were $E_{pa}$ (V) = 0.712 - 0.0568 pH ($R^2$ = 9898) for DA, $E_{pa}$ (V) = 0.532 - 0.0512 pH ($R^2$ = 9987) for UA, $E_{pa}$ (V) = 0.91 - 0.0316 pH ($R^2$ = 9917) for Trp and $E_{pa}$ (V) = 1.3016 - 0.0392 pH ($R^2$ = 9961) for TP. The slopes of DA and UA approached 59 mV $pH^{-1}$ (the theoretical value), which proves that the number of transferred protons was equivalent to the number of electrons. The slopes of the linear

regression lines of Trp and TP both approached the 1/2 theoretical value, so the proton transfer number in the reaction process was half of the electron transfer number [45].

Fig. 8C reveals the effect of pH on the peak currents. The peak currents of Trp and TP decreased inch by inch when the pH became alkaline, while $I_{DA}$ and $I_{UA}$ reached their maximum values at pH = 6.0. In summary, in subsequent experiments, pH = 6.0 was selected as the best detection condition.

### *3.5.3. The influence exerted by scan rate*

The behavior of the four biomolecules was studied using CV at different scanning rates (10 - 230 mV/s) (Figs. 9A-D). Figs. 9E-F show that $I_{DA}$, $I_{UA}$, $I_{Trp}$ and $I_{TP}$ were proportional to the square root of the scan rate. According to the electrode reaction kinetics, all electrode reactions of these four analytes were diffusion-controlled processes.

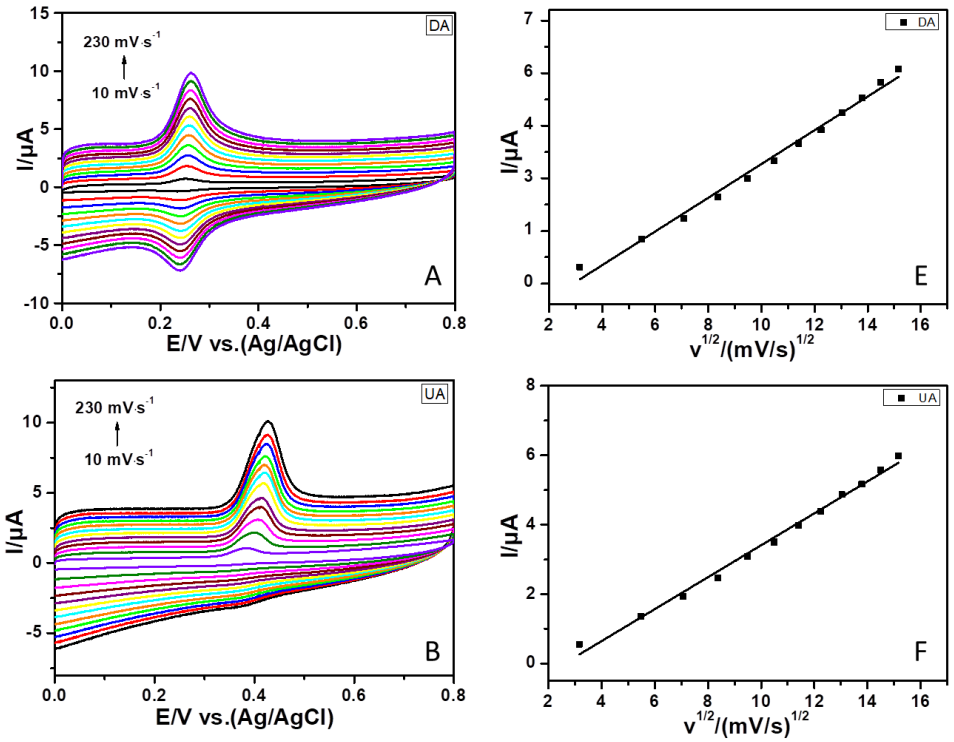

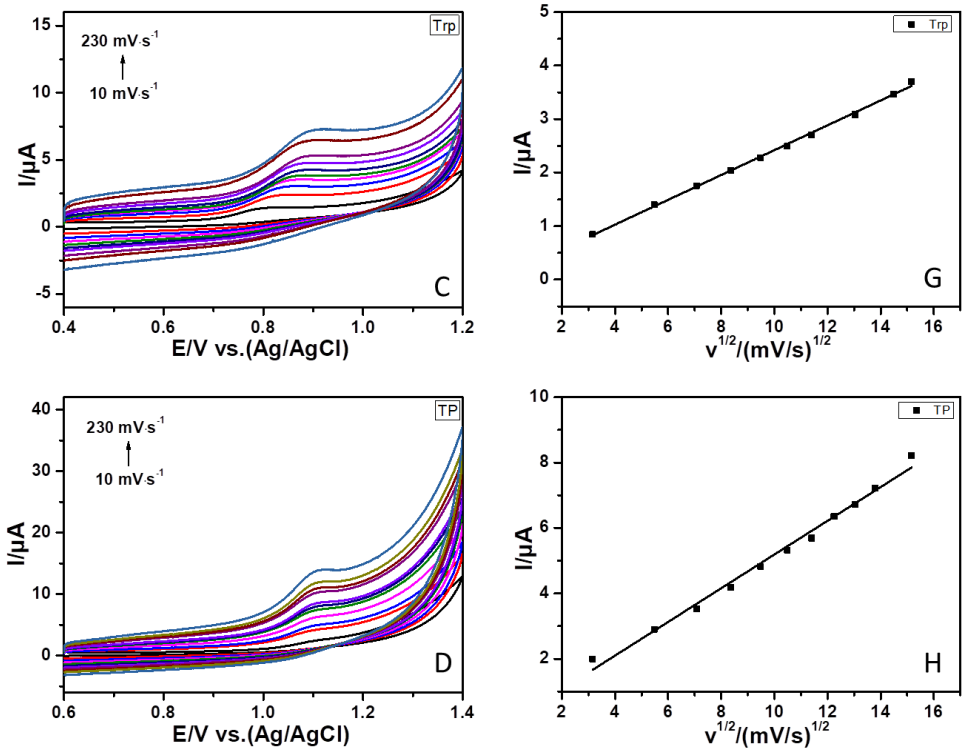


**Figure 9.** (A-D) CVs obtained from 20 μM DA, 40 μM UA, 50 μM Trp and 50 μM TP at various scan rates (10-230 mV/s); (E-H) I vs. $v^{1/2}$ $(mV/s)^{1/2}$ .

*3.6. Simultaneous and individual determination of DA, UA, Trp and TP*

Fig. 10 shows the DPV curve obtained by concurrently changing the concentrations of the four selected biomolecules in the mixture. The peak currents linearly increased when their concentration gradient changed.

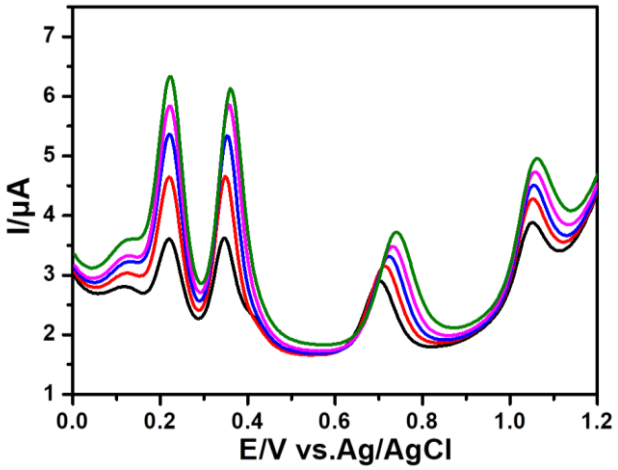


**Figure 10.** DPVs obtained from DA (1 - 5 μM), UA (30 - 50 μM), Trp (10 - 50 μM) and TP (60 - 100 μM) on CDs/GCE.

Simultaneous analysis of the four biomolecules was accomplished by DPV. Their signal intensity was portrayed by altering the concentration of one biomolecule, while the other three were invariant (Fig. 11). In Fig. 11A, the change in DA concentration from 0.5 μM to 50 μM made $I_{DA}$ linearly increase, while $I_{UA}$, $I_{Trp}$ and $I_{TP}$ remained constant. Furthermore, the respective changes in UA concentration from 3 μM to 75 μM, Trp concentration from 1 μM to 65 μM and TP concentration from 10 μM to 200 μM were recorded (Fig. 11B-D). The peak currents of the other three species remained stable.

Based on the linear results, the following regression equations were reached:

$I_{DA}$ (μA) = 0.7214 $C_{DA}$ (μM) + 0.7530 ($R^2$ = 0.9988) (Fig. 11A)

$I_{UA}$ (μA) = 0.0528 $C_{UA}$ (μM) + 0.2254 ($R^2$ = 0.9980) from 3 μM to 28.5 μM and $I_{UA}$ (μA) = 0.1947 $C_{UA}$ (μM) – 4.2658 ($R^2$ = 0.9898) from 28.5 μM to 75 μM. (Fig. 11B)

$I_{Trp}$ (μA) = 0.0616 $C_{Trp}$ (μM) + 0.0933 ($R^2$ = 0.9912) from 1 μM to 15 μM and $I_{Trp}$ (μA) = 0.0298 $C_{Trp}$ (μM) + 0.5678 ($R^2$ = 0.9977) from 15 μM to 65 μM. (Fig. 11C)

$I_{TP}$ (μA) = 0.0170 $C_{TP}$ (μM) + 0.9653 ($R^2$ = 0.9989) (Fig. 11D)

Their LODs were 0.007 μM for DA, 0.011 μM for UA, 0.11 μM for Trp, and 0.33 μM for TP (S/N = 3).

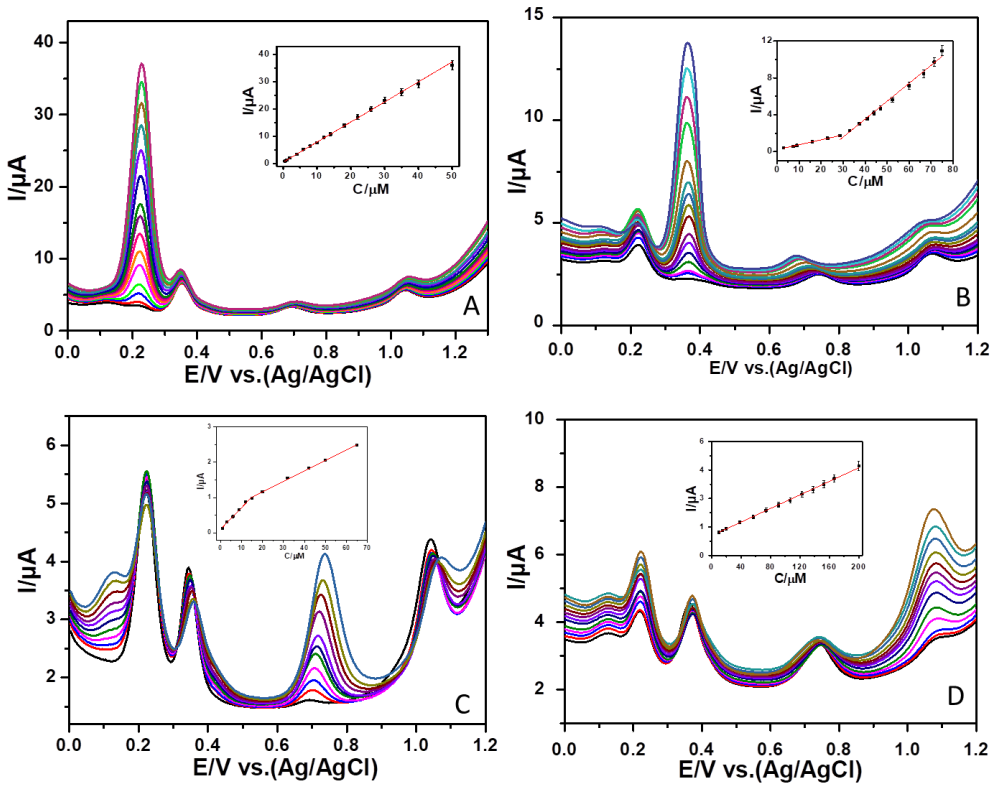


**Figure 11.** (A) DPVs at CDs/GCE of DA with various concentrations in the mixture (pH 6.0); (B) DPV at CDs/GCE of UA with various concentrations in the mixture (pH 6.0); (C) DPV at CDs/GCE of Trp with various concentrations in the mixture (pH 6.0); (D) DPV at CDs/GCE of TP with various concentrations in the mixture (pH 6.0).

*3.7. Interference studies*

The mixed solution contained four biomolecules and various potential interferences, which contained inorganic salts (such as 50 mM $NH_4^+$, $Cl^-$, $SO_4^{2-}$, $NO_3^-$, $K^+$ and 100 mM $Na^+$), amino acids (such as 5 mM alanine (Ala), L-phenylalanine (L-phe) and L-valine (L-val)), 50 μM ascorbic acid (AA), 5 mM citric acid (CA) and glucose (Glu), which were successively added to PBS (pH 6.0) and recorded using chronoamperometry.

As shown in Fig. 12, when 9 interfering substances were added to the solution, no new signals were detected. The subsequent addition of solution increased the volume of the original solution, which slightly decreased the concentrations of DA, UA, Trp and TP, and the signal was weakened. However, when the four biomolecules were added once more, a strong current signal immediately appeared. The experimental results reveal that the prepared electrode had strong anti-interference performance and excellent selectivity in nonenzymatic catalysis.

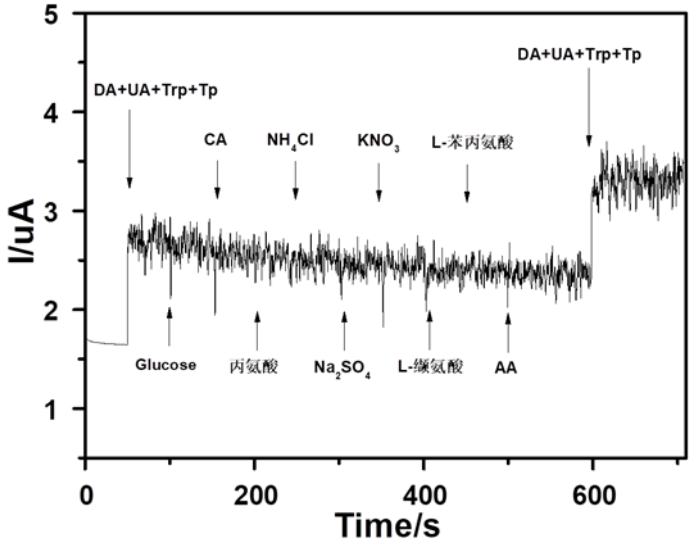


**Figure 12.** Chronoamperometry of a successively added mixture of 5 μM DA, 20 μM UA, 20 μM Trp, 20 μM TP and potential disruptors including 50 mM $NH_4^+$, $Cl^-$, $SO_4^{2-}$, $NO_3^-$, $K^+$, 100 mM $Na^+$, 5 mM CA, Glu, Ala, L-val, L-Phe and 50 μM AA at 1.10 V on CDs/GCE in PBS (pH 6.0).

*3.8. Reproducibility, repeatability and stability studies*

Within half a month (stored in refrigerator), the current density of the four biomolecules decreased by 0.73%, 8.2%, 7.1% and 3.0% compared to the original signals in PBS (pH 6.0). The good performance of the proposed electrode after a storage period indicates its good stability.

Nine consecutive measurements were performed using the same CDs/GCE to simultaneously identify four biomolecules with a relative standard deviation (RSD) of 6.8% for DA, 6.2% for UA, 7.2% for Trp and 7.0% for TP. Five CDs/GCE were obtained to identify these four biomolecules with an RSD less than 7.1%. These data confirm the repeatability and reproducibility of the prepared

electrode.

**Table 1**. Comparison with various biosensors.

| Biosensors | Linear range (μM) | | | | Detection limit (μM) | | | | Ref |
|---|---|---|---|---|---|---|---|---|---|
| | DA | UA | Trp | TP | DA | UA | Trp | TP | |
| (Au-PDNs)/GCE | 1-160<br>160-350 | 1-120<br>120-350 | 1.0-160<br>160-280 | \ | 0.0001 | 0.0001 | 0.0001 | \ | [46] |
| GC/MWCNT-FeNAZ-CH | 7.35-833 | 0.23-83.3 | 0.074-34.5 | \ | 1.05 | 0.033 | 0.011 | \ | [47] |
| GNPs/PImox/GCE | 5.0-268.0 | 6.0-486.0 | 3.0-34.0<br>84.0-464.0 | \ | 0.08 | 0.5 | 0.7 | \ | [48] |
| MWCNs/MGF/GCE | 0.3-10 | 5-100<br>300-1000 | 5-30<br>60-500 | \ | 0.06 | 0.93 | 0.87 | \ | [49] |
| AT/AuNPs/GCE | \ | 0.03-100 | \ | 0.04-100 | \ | 0.061 | \ | 0.000076 | [50] |
| pPABSA/GCE | \ | 10-80 | \ | 10-100 | \ | 0.1 | \ | 7.02 | [51] |
| Fe-Meso-PANI | 10-300 | 10-300 | 10-300 | \ | 9.8 | 5.3 | 5.2 | \ | [52] |
| GS–PTCA/GCE | 0.40-374 | 4-544 | 0.40-138 | \ | 0.13 | 0.92 | 0.06 | \ | [53] |
| β-CD/CQDs/GCE | 4-220 | 0.3-200 | 5-270 | \ | 0.14 | 0.01 | 0.16 | \ | [15] |
| Hand-in-hand RNA nanowire | \ | \ | \ | 0.5-70 | \ | \ | \ | 0.05 | [54] |
| poly-Gly/GPE | 0.3-60 | 0.4-105 | \ | \ | 0.089 | 0.1 | \ | \ | [55] |
| 1,4-BBFT/Carbon paste | \ | \ | \ | 0.06-700 | \ | \ | \ | 0.012 | [56] |
| multiwall carbon nanotube/GCE | \ | \ | \ | 0.3-10 | \ | \ | \ | 0.05 | [57] |
| Nitrogen doped grapheme/GCE | 0.5-170 | 0.1-20 | \ | \ | 0.25 | 0.045 | \ | \ | [58] |
| poly(CTAB)/GCE | 0.50-1000 | 1.0-1000 | 1.0-1000 | 0.50-1000 | 0.11 | 0.33 | 0.44 | 0.11 | [19] |
| CDs/GCE | 0.5-50 | 3-28.5<br>28.5-75 | 1-65 | 10-200 | 0.007 | 0.011 | 0.11 | 0.33 | This work |

*3.9. Human serum analysis*

To further understand the usefulness of CDs/GCE in real sample detection, DA, UA, Trp and TP were detected in human serum. According to the standard addition method, 0.1 mL of human serum was added to the standard solution and measured (DPV). Data were summed up and sorted in Table 2. The recovery rate was determined by multiplying the ratio of the theoretical concentration to the actual concentration by 100%.

**Table 2**. Testing data of human serum.

| Sample | Serum (μM) | | | | Added (μM) | | | | Founded (μM) | | | | Recovery (%) | | | |
|---|---|---|---|---|---|---|---|---|---|---|---|---|---|---|---|---|
| | DA | UA | Trp | TP | DA | UA | Trp | TP | DA | UA | Trp | TP | DA | UA | Trp | TP |
| 1 | 0 | 2.59 | 1.43 | 0 | 3.50 | 20.00 | 6.00 | 35.00 | 3.32 | 21.70 | 7.07 | 35.68 | 94.95 | 95.57 | 94.00 | 101.9 |
| 2 | 0 | 3.78 | 1.57 | 0 | 4.50 | 25.00 | 12.00 | 55.00 | 4.56 | 26.81 | 13.53 | 55.98 | 101.5 | 92.14 | 99.67 | 101.8 |
| 3 | 0 | 0.61 | 0.13 | 0 | 5.50 | 30.00 | 18.00 | 75.00 | 5.45 | 30.74 | 17.39 | 74.09 | 99.17 | 100.4 | 95.88 | 98.79 |

## 4. CONCLUSIONS

CDs prepared by one-step ultrasonic technology with glucose as the carbon source were equally distributed on the GCE. Four weak and partially overlapped signals of DA, UA, Trp, and TP were significantly amplified into four well-identified oxidation peaks due to their good biocompatibility. This simple electrode was directly used to discriminate the four analytes in the presence of coexisting interferences in biological fluids. It provided a promising strategy to selectively discriminate these four biomolecules in human serum with outstanding anti-interference ability.

ACKNOWLEDGEMENT
This study was supported by the National Natural Science Foundation of China (No. 21575160).

## References

1. Z. Wang, J. Liu, Q. Liang, Y. Wang and G. Luo, *Analyst*, 127 (2002) 653.
2. J. Huang, Y. Liu, H. Hou and T. You, *Biosens. Bioelectron.*, 24 (2008) 632.
3. Y. Li and X. Lin, *Sens. and Actuators B-Chem.*, 115 (2006) 134.
4. Y.J. Yang and W. Li, *Biosens. Bioelectron.*, 56 (2014) 300.
5. B. Kaur, T. Pandiyan, B. Satpati and R. Srivastava, *Colloids and surfaces. B, Biointerfaces*, 111 (2013) 97.
6. S. Tajik, M.A. Taher and H. Beitollahi, *Sens. Actuators B-Chem.*, 197 (2014) 228.
7. C. Xue, Q. Han, Y. Wang, J.H. Wu, T.T. Wen, R.Y. Wang, J.L. Hong, X.M. Zhou and H.J. Jiang,

*Biosens. Bioelectron.*, 49 (2013) 199.
8. Q. Huang, X. Lin, C. Lin, Y. Zhang, S. Hu and C. Wei, *Rsc. Adv.*, 5 (2015) 54102.
9. B.F. Culleton, M.G. Larson, W.B. Kannel and D. Levy, Ann. Intern. Med., 131 (1999) 7.
10. M.A. Raj, S.A. John, *Anal. chimi. Acta*, 771 (2013) 14.
11. C. Herve, P. Beyne, H. Jamault and E. Delacoux, *J. Chromatography B*, 675 (1996) 157.
12. R.D. Thompson, H.T. Nagasawa and J.W. Jenne, *Transl. Res.*, 84 (1974) 584.
13. M.J. Cooper, B.L. Mirkin and M.W. Anders, *J. Chromatogr.*, 143 (1977) 324.
14. O. Brors, G. Sager, D. Sandnes and S. Jacobsen, *Brit. J.Clin. Pharmaco.* 15 (1983) 393.
15. J. Chen, P. He, H. Bai, S. He, T. Zhang, X. Zhang and F. Dong, *Sens. Actuator B-Chem.*, 252 (2017) 9.
16. L. Yang, N. Huang, Q. Lu, M. Liu, H. Li, Y. Zhang and S. Yao, *Anal. chim. Acta*, 903 (2016) 69.
17. Y. Zhang, Z. Xia, H. Liu, M. Yang, L. Lin and Q. Li, *Sens. Actuator B-Chem.*, 188 (2013) 496.
18. L. Sun, H. Li, M. Li, P. Li, C. Li and B. Yang, *J. Electrochem. Soc.*, 163 (2016) B567.
19. Y.J. Yang, L. Guo and W. Zhang, *J. Electroanal. Chem.*, 768 (2016) 102.
20. X. Ding, Y. Niu, G. Zhang, Y. Xu and J. Li, *Chem. Asian J.*, 15 (2020) 1214.
21. Y.F. Wang and A.G. Hu, *J. Mater. Chem. C*, 2 (2014) 6921..
22. S. He, P. He, X. Zhang, X. Zhang, F. Dong, L. Jia, L. Du and H. Lei, *Mikrochim. Acta*, 185 (2018) 107.
23. L. Cao, X. Wang, M.J. Meziani, F.S. Lu, H.F. Wang, P.J.G. Luo, Y. Lin, B.A. Harruff, L.M. Veca, D. Murray, S.Y. Xie and Y.P. Sun, *J. Amer. Chem. Soc.*, 129 (2007) 11318.
24. V. Mishra, A. Patil, S. Thakur and P. Kesharwani, *Drug Discov. Today*, 23 (2018) 1219.
25. C. Liu, P. Zhang, X. Zhai, F. Tian, W. Li, J. Yang, Y. Liu, H. Wang, W. Wang and W. Liu, *Biomaterials*, 33 (2012) 3604.
26. K.G. Qu, J.S. Wang, J.S. Ren and X.G. Qu, *Chem-Eur J.*, 19 (2013) 7243.
27. C. Wei, Q. Huang, S. Hu, H. Zhang, W. Zhang, Z. Wang, M. Zhu, P. Dai and L. Huang, *Electrochim. Acta*,149 ( 2014) 237.
28. Y. Wei, Z. Xu, S. Wang, Y. Liu, D. Zhang and Y. Fang, *Ionics*, 26 (2020) 5817.
29. R.M. Shereema, T.P. Rao, V.B. Sameer Kumar, T.V. Sruthi, R. Vishnu, G.R.D. Prabhu and S. Sharath Shankar, *Mat. sci.eng. C-Mater.*, 93 (2018) 21.
30. J. Wang, H. Zhang, J. Zhao, R. Zhang, N. Zhao, H. Ren and Y. Li, *Microchim. Acta*, 186 (2019) 733.
31. W. Zhang, J. Zheng, Z. Lin, L. Zhong, J. Shi, C. Wei, H. Zhang, A. Hao and S. Hu, *Anal. Methods*, 7 (2015) 6089.
32. D. He, S. Li, P. Zhang and H. Luo, *Anal. Methods*, 9 (2017) 6689.
33. H. Li, X. He, Y. Liu, H. Huang, S. Lian, S.-T. Lee and Z. Kang, *Carbon*, 49 (2011) 605.
34. R. Karthikeyan, D.J. Nelson and S.A. John, *Anal. Methods*, 11 (2019) 3866.
35. C.Q. Wang, J. Du, H.W. Wang, C.E. Zou, F.X. Jiang, P. Yang and Y.K. Du, *Sens. Actuator B-Chem.*, 204 (2014) 302.
36. Q. Xiao, S. Lu, C. Huang, W. Su and S. Huang, *Sensors*, 16 (2016) 1874.
37. S. Campuzano, P. Yanez-Sedeno and J.M. Pingarron, *Nanomaterials*, 9 (2019) 634.
38. Y.P. Sun, B. Zhou, Y. Lin, W. Wang, K.A.S. Fernando, P. Pathak, M.J. Meziani, B.A. Harruff, X. Wang, H.F. Wang, P.J.G. Luo, H. Yang, M.E. Kose, B.L. Chen, L.M. Veca and S.Y. Xie, *J. Amer. Chem. Soc.*, 128 (2006) 7756.
39. W. Guo, F. Pi, H. Zhang, J. Sun, Y. Zhang and X. Sun, *Biosens. Bioelectron.*, 98 (2017) 299.
40. M. Baghayeri, M. Namadchian, H. Karimi-Maleh and H. Beitollahi, *J. Electroanal. Chem.*, 697 (2013) 53.
41. N. Hoai Viet, L. Richtera, A. Moulick, K. Xhaxhiu, J. Kudr, N. Cernei, H. Polanska, Z. Heger, M. Masarik, P. Kopel, M. Stiborova, T. Eckschlager, V. Adam and R. Kizek, *Analyst*., 141 (2016) 2665.
42. A.a.M. Noor, M.M. Shahid, P. Rameshkumar, N.M. Huang, *Microchim. Acta.*, 183(2) (2016) 911.
43. A.E. Bolzan, *Electrochim. Acta.*, 113 (2013) 706.

44. G. Jiang, T. Jiang, H. Zhou, J. Yao and X. Kong, *Rsc. Adv.*, 5 (2015) 9064.
45. E. Laviron, *J. Electroanal. Chem.*, 164(1984) 213.
46. A. Arroquia, I. Acosta and M.P.G. Armada, *Mater. Sci. Eng. C-Mater. Biol. Appl.*, 109 (2020) 10.
47. M. Noroozifar, M. Khorasani-Motlagh, R. Akbari and M.B. Parizi, *Biosens. Bioelectron.* 28(2011) 56.
48. C. Wang, R. Yuan, Y. Chai, S. Chen, F. Hu and M. Zhang, *Anal. Chim. Acta*, 741 (2012) 15.
49. H.X. Li, Y. Wang, D.X. Ye, J. Luo, B.Q. Su, S. Zhang and J.L. Kong, *Talanta*, 127 (2014) 255.
50. S. Kesavan, S.A. John, *Sens. Actuator B-Chem.*, 205 (2014) 352.
51. S. Jesny and K.G. Kumar, *Electroanalysis*, 29 (2017) 1828.
52. M.U.A. Prathap and R. Srivastava, *Sens. Actuator B-Chem.*, 177 (2013) 239.
53. W. Zhang, Y.Q. Chai, R. Yuan, S.H. Chen, J. Han and D.H. Yuan, *Anal. chim. Acta*, 756 (2012) 7.
54. J. Wang, W.B. Cheng, F.Y. Meng, M. Yang, Y. Pan and P. Miao, *Biosens. Bioelectron.*, 101 (2018) 153.
55. Y. Zhang, *Int. J. Electrochem. Sci.*, 15(2020) 11387.
56. S. Tajik, M.A. Taher and H. Beitollahi, *Sens. Actuator B-Chem.*, 197 (2014) 228.
57. Y.H. Zhu, Z.L. Zhang, D.W. Pang, *J. Electroanal. Chem.*, 581 (2005) 303.
58. Z.H. Sheng, X.Q. Zheng, J.Y. Xu, W.J. Bao, F.B. Wang and X.H. Xia, *Biosens. Bioelectron.*, 34 (2012) 125